Oxidation and Stabilization of Unreconstructed Hydrogen- and Fluorine-Terminated Si(100) Surface: A Periodic Density Functional Study

Abhijit Chatterjee,* Takashi Iwasaki, and Takeo Ebina

Inorganic Materials Section, Tohoku National Industrial Research Institute, 4-2-1 Nigatake, Miyagino-ku, Sendai 983-8551, Japan

Momoji Kubo and Akira Miyamoto

Department of Materials Chemistry, Graduate School of Engineering, Tohoku University, Sendai 980-8579, Japan

Received: June 24, 1998; In Final Form: August 26, 1998

The understanding and control of silicon surfaces is of great importance in the production of silicon-based electronic devices made from semiconductor materials and constructed on silicon single-crystal substrates. This is the first study to see the effect of surface etching by fluorine on the stability of the unreconstructed Si(100) surface using periodic density functional calculations. All the possible fluorine substitution sites are considered, and the results are compared with the existing experimental observation in terms of suitability of fluorine substitution on the surface. The results are compared with H-terminated surfaces to prove the efficiency of fluorine in stabilizing the unreconstructed Si(100) surface. Oxidation of the Si(100) surface for both H- and F-terminated surfaces were also studied to propose the plausible mechanism of oxidation. Two kinds of experimental situations were mimicked for oxidation; (1) oxidation on the surface, i.e., generation of the Si−O−H bond, and (2) oxidation on the bridging bond between two silicons, i.e., generation of Si−O−Si, were compared to show the feasibility of Si−O−Si bond formation. Oxidation through atomic oxygen was followed throughout the calculation. The calculations were performed with smaller clusters using density functional methodology to validate and rationalize the current understanding. The results were further supported by molecular electrostatic potential maps generated from periodic density functional calculation results.

Introduction

The adsorption of oxygen on Si(100) has been the object of many studies for several years.[1] Indeed it is a fundamental matter in semiconductor technology.[2,3] Silicon is the most used semiconductor because of the good quality of its oxide.[4] A better knowledge of the microscopic structure would help to improve the performance of electronic devices in reducing the thickness of the metal-oxide-semiconductor gate of the complementary metal oxide semiconductor (CMOS) transistors. The thickness of oxide film used as a gate dielectric in metal-oxide-semiconductor field effect transistors (MOSFET) corresponds to a few to 10 molecular layers. Atomic scale control of the oxidation process is therefore an urgent task in the semiconductor industry. Because the thickness of the gate oxide is comparable to the native oxide formed on a clean surface, use of surfaces on which active dangling bonds are saturated with hydrogens has been studied by using different experimental techniques, e.g., atomic force microscopy,[5] scanning tunneling microscopy,[6] and high-resolution electron energy loss spectroscopy.[7] One of the aims of this study of oxidation of the Si(100) surface is thus to determine a possible oxygen monolayer structure which could be at the silicon−silica interface.[8] The dissociation on the surface is exothermic. There are different propositions about oxygen adsorption on the Si surface both for molecular and atomic oxygen. Although O_2 has a very short lifetime above 90 K and thus is difficult to isolate, atomic adsorption is obtained. O_2 adsorption might be present when the most active sites are already covered by O. Then a small amount of molecularly adsorbed dioxygen may coexist with atomic oxygen.[9] On the contrary O_2 adsorption might be a metastable precursor for the dissociative adsorption as supported by spectroscopic results. From theoretical calculation O_2 is predicted to adsorb dissociatively.[10] Initial adsorption of both molecular and atomic oxygen was found to lead to the insertion of O into dimer bond as observed by the first principle calculation. There now seems to be a general consensus derived from both theoretical cluster calculations[11−13] and experiment[14,15] that the initial oxidation of the Si(100) surface is via dissociative chemisorption, these calculations have been restricted to the cause of atomic adsorption. We have chosen a unreconstructed Si(100) surface for the study, and the atomic oxygens are allowed to interact with both surface and bridging silicons with hydrogen termination. Molecular halogens are chemisorbed on the Si(100) surface exothermally and form a stable adsorbed structure on the Si(100) surface at low temperatures.[16] The halogen atoms are chemically bonded dimer dangling bonds or bonded on bridge sites. A flux of halogen atoms and molecules exposed to Si surfaces at elevated temperatures also yields a continuous etching of the Si surfaces. The interaction of fluorine with silicon has attracted particular interest because of its fundamental role in the processing of microelectronic devices.[17−20] Etching of silicon wafers often uses plasmas of fluorine-containing molecules, where the primary reactive species is thought to be F atoms.[21] Upon initial fluorine exposure, rapid

* Corresponding author: E-mail: chatt@tniri.go.jp. Phone: +81-22-237-5211. Fax: +81-22-236-6839.

10.1021/jp982758z CCC: $15.00
Published on Web 10/22/1998

adsorption of 1.5 monolayers (ML) of F occurs.[22] Continuous exposure then leads to a buildup of a fluorosilyl layer consisting of SiF, SiF_2, and SiF_3.[23−25] The adsorption and reaction of both molecular and atomic fluorine with the Si(100) surface has been examined by Engstrom et al.[26] under ultrahigh vacuum conditions with supersonic molecular beam techniques, X-ray photoelectron spectroscopy, quadrupole mass spectrometry, and low-energy, ion-scattering spectroscopy. They observed that adsorption of atomic F is qualitatively distinct from molecular fluorine. The adsorption probability of F(g) exceeds that for F_2(g) by approximately 2 orders of magnitude. In addition, unlike molecular F, the adsorption of atomic F at high coverages may be activated. They also predict that the steady-state reaction between F_2(g) and Si(100) surface involves a reaction between chemisorbed F atoms, which results from the dissociative adsorption of F_2 and Si substrates. The high-pressure kinetic data suggest that dissociative adsorption via an extrinsic precursor is important in the steady-state etching of Si by F_2 molecules. There are many experimental studies relating the surface etching of Si.[27,28] There are also a few theoretical, mainly molecular dynamics studies on the etching process. Using molecular dynamics, an initial adsorption probability of unity is observed,[29] whereas S = 0 for an ordered F monolayer. In long time simulations, beginning of the buildup of the fluorosilyl layer, with Si−Si dimer bond breaking occurring simultaneously with Si dangling bond saturation, is also observed. In another study with ab initio derived molecular dynamics,[30] it was pointed out that many different paths of reaction are competing e.g., fluorination of dangling bonds, breaking of dimer bonds, and attack of subsurface Si atoms. This leads to the concurrent formation of adsorbed SiF, SiF_2, and SiF_3. The large exothermicity of the reaction caused by the tremendous strength of the Si−F bonds results in a local heating effect that introduces disorder in the lattice, weakening existing bonds and exposing new dangling bonds. The ordered surfaces with coverages of one monolayer of F or more are not reactive because of the formation of an impenetrable layer of F atoms on the surface. With this background we propose to study first the surface reaction of fluorine followed by comparison of the oxidation of the unreconstructed Si(100) surface for both clean and fluorinated systems. The layer density is maintained to a monolayer only. Insertion of oxygen into the bridge sites between the first and second layer was compared for both situations. A plausible oxidation mechanism has been rationalized.

Method and Model

Periodic density functional calculations were performed using DSOLID code of MSI Inc.[31] applying Kohn−Sham formalism.[32] One-electron Schrodinger wave equations were solved only at K = 0 wave vector point in the Brilloin zone. The Vasko−Wilk−Nusair local-type functional[33] was used in this calculation. The electronic orbitals within a unit cell were composed of linear combinations of numerically tabulated atomic orbitals.[34] The size of the basis set was double numerical with polarization functions (DNP). Test calculations showed no sign of the dangerous linear dependencies often associated with linear combination of atomic orbitals basis sets in periodic calculations.[35] The numerical integrations were performed on a grid of medium-quality mesh size. The core orbitals of the atoms were necessarily frozen to reduce central processing unit (CPU) time. The crystal electrostatics of the nuclei and the continuous electronic charge distribution were computed by a modified Ewald method[36] as described in detail in ref 37. The final

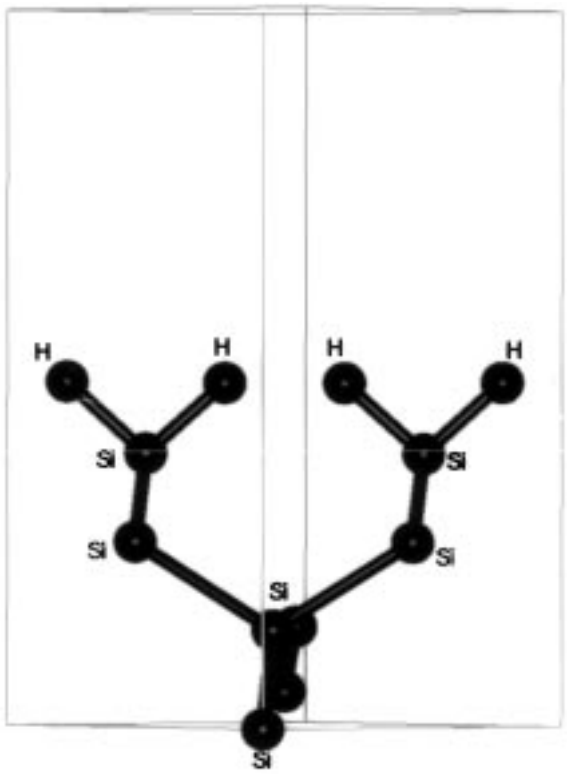

Figure 1. The periodic model for the H-terminated unreconstructed Si(100) surface.

geometries were accepted when the norm of the energy gradient was less than 0.002 au. At the optimized structure nonlocal functionals were used to get the energy at the self-consistent field level. The adsorption energies were calculated according to the expression: $E_{ads} = E_O + E_{slab} - E_{(O+slab)}$, where $E_{(O+slab)}$ is the total energy of the optimized oxidized slab, E_O is the unrestricted energy of the atomic oxygen, and E_{slab} is the energy of the optimized slab.

The Si(100) surface model was generated from bulk consisting of 12 atoms including 8 Si and 4 H. Our model of the Si(100) surface is a slab consisting of four layers of Si atoms. The model is shown in Figure 1; the hydrogens at the Si termination have not been shown due to better visibility. In this model all the dangling bonds both at the bottom and top are saturated with hydrogens. The Si−H distance is 1.48 Å. The length of the actual cell along the surface normal vector is 20 Å, which is sufficient for surface modeling. In addition to periodic calculations, we present results with molecular models performed at the same level of accuracy. These calculations were performed to serve two purposes: (1) to generate optimized structures to be transferred to periodic calculation and (2) to support the geometry of adsorbed species by providing a system simpler to analyze. We have used a model in which a couple of SiH_3 radicals generate two dangling bonds as in the space between two Si of the surface. Two models were considered: SiH_3−SiH_3 and SiH_2=SiH_2. In this model, the Si−Si distance is usually large. These models are expected to illustrate the insertion for the unreconstructed surface. These models will be used as a reference to understand the binding modes. We have made the calculations for the model without polarization functions, because the calculations for the slab have low symmetry. Molecular electrostatic potential (MESP) was calculated using the methodology described elsewhere.[38]

Results and Discussion

Periodic density functional calculations were initially performed on a clean surface to test the validity of the model by comparing the geometric parameters with experimental observation. This was followed by the calculation of the effect of H and F termination on various possible models of F termination over the Si(100) surface. We compared the stabilization energy of different models to compare the effect of termination on the stability of the Si(100) surface. After this the oxidation of both H- and F-terminated surfaces was tested. For H-terminated surfaces the situations with Si−O−H on the surface and Si−O−Si at the bridge were compared, whereas for the F-terminated surface, only the Si−O−Si bridge was tested. The stabilization energies for all the models were compared. The constraint of the model is that the first-layer Si was kept fixed throughout the calculation. The results were further compared with the experimental prediction. The results of the periodic calculations were also tested with the trend produced by cluster calculations using density functional theory (DFT). The cluster calculations were aimed to justify the atomic oxygen adsorption on the surface and to rationalize the binding modes.

(a) Validity of the Calculation. To evaluate the validity of our calculations, we first performed calculations on the clean surface. We found that the unreconstructed surface was not metallic. The band gap calculated from the difference of occupation in molecular orbitals at one k point represents 3.6 eV. The lowest unoccupied band has a 2px character localized on the surface atoms, whereas the highest occupied band has predominantly 2s and 2pz character. The fermi level calculated for the unreconstructed surface is 0.254 au. Real surface is also not metallic as shown by photoemission spectroscopy.[39] Most of the theoretical calculations[40] find that the symmetric dimer is metallic and that the buckling is necessary to open a gap. It is known that density functional approximation underestimates the band gaps of semiconductors,[41] whereas Hartree−Fock usually overestimates them.[42,43] The geometric parameters also match with experimental findings as follows (the experimental value is written in the parentheses): Si−H 1.47 Å (1.48 Å); Si−Si 2.29 Å (2.35 Å); Si−Si−Si angle in the layers 110.92 (109.47). This justifies the choice of the periodic model.

(b) Effect of Termination on the Stability of the Unreconstructed Si(100) Surface. First, we optimized the H-terminated surface with the model shown in Figure 1. It is observed that the Si−H optimized bond length is 1.47 Å, which is in close agreement with the experimentally observed value of 1.48 Å. The interlayer Si−Si distances are 2.29 Å on average. These results justify our model. In the analogy with the surface, SiH_2 represents the site of the unreconstructed surface; it does not possess dangling bonds equally populated, the σz orbitals normal to the surface are occupied, and the 2px orbitals parallel to the surface are vacant. Experimentally, the $^1A_1$ state is lower than the $^3B_1$ state by 21 kcal/mol; this result, opposite to that of CH_2, is also found by more accurate calculations.[44,45] The difference between the singlet and triplate states is consistent with the nonmetallic character found for the periodic calculation.

Next, we generated a different model with F as described in the following sequence: (1) 1F on the Si(100) surface with the remaining three H named as F−H−H−H; (2) 2F on different Si in a different direction on the top layer of the Si(100) surface alternatively named as H−F−H−F. (This model is shown in Figure 2.); (3) 2F on same Si on the top layer of Si(100) surface named as F−F−H−H; (4) 2F with different top Si in same direction on the top layer of the Si(100) surface occurring continuously named as H−F−F−H. This model is shown in Figure 3.

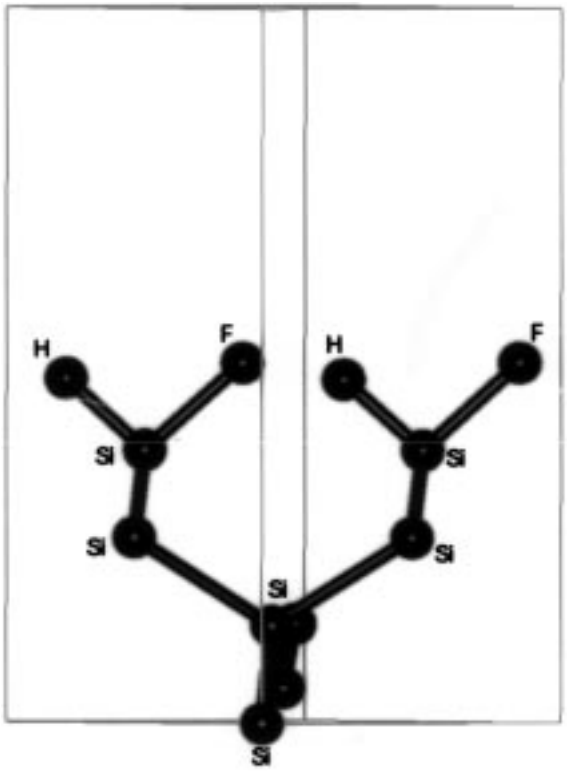

Figure 2. Two F on different Si in different directions on the top layer of the unreconstructed Si(100) surface occurring alternately and named as H−F−H−F.

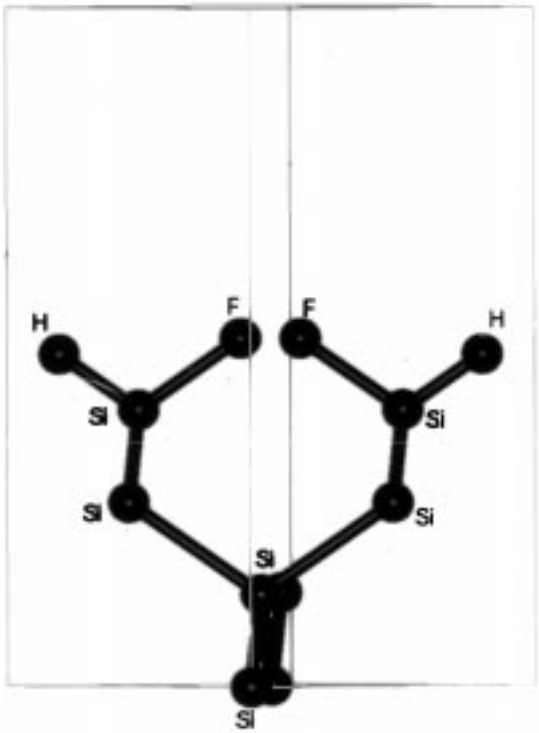

Figure 3. Two F on different Si in same direction on the top layer of the unreconstructed Si(100) surface, occurring one after another and named as H−F−F−H.

The model structure, as shown in Figure 1, consists of all hydrogens on the unreconstructed Si(100) surface. The binding

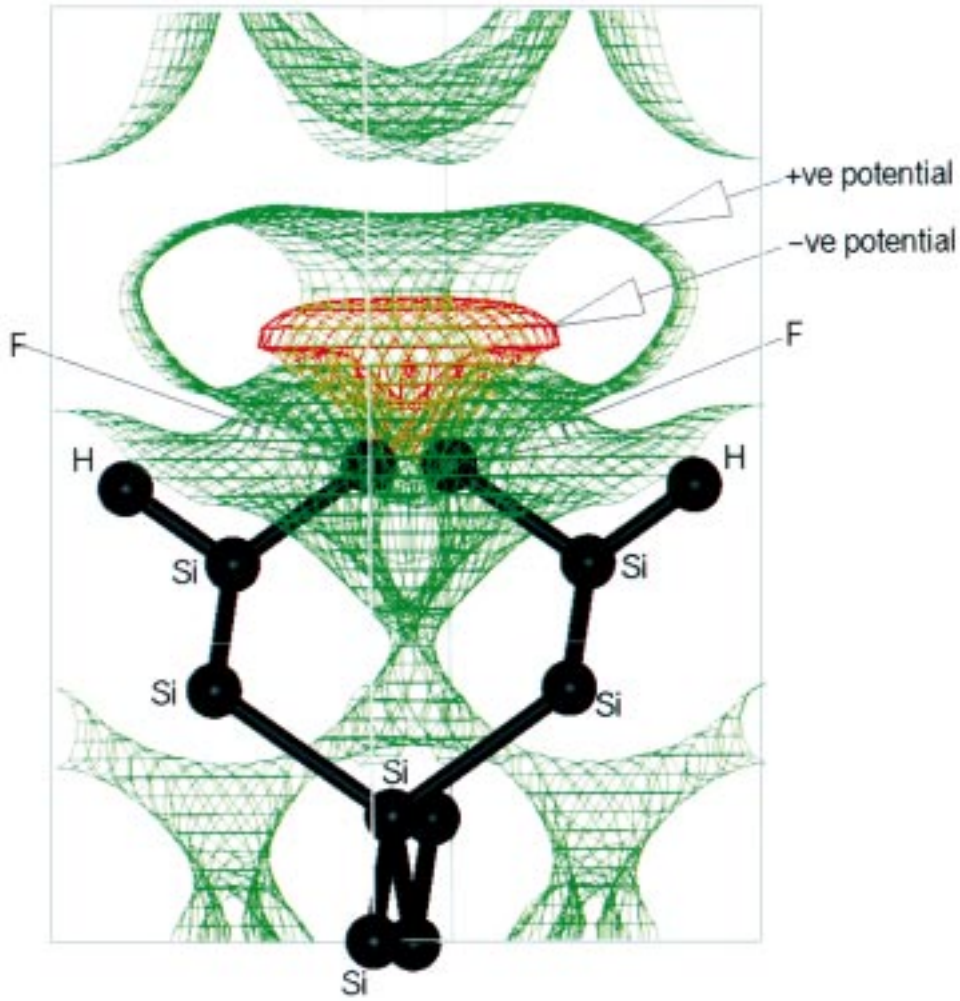

Figure 4. MESP map for the unreconstructed Si(100) surface model H−F−F−H. The +ve and −ve potentials are shown as green and red shades, respectively. The −ve potential values in the range of −0.05 au to 0.00 au and the positive potentials in the range of 0.00 to 0.05 au are shown.

TABLE 1: Comparison of Binding Energy and Relative Stabilization Energy of the Respective Models of Unreconstructed Si(100) Surface

surface models	binding energy (eV)	relative stabilization energy (eV)
H−H−H−H	−42.69	10.30
F−H−H−H	−46.24	6.76
H−F−F−H	−48.09	4.91
F−F−H−H	−48.53	4.47
H−F−H−F	−53.00	0

energy and the relative stabilization energies for all the individual models are calculated and shown in Table 1. The results show the following order of the models in terms of stabilization of the Si(100) surface:

$$\text{H−F−H−F} > \text{F−F−H−H} > \text{H−F−F−H} > \text{F−H−H−H} > \text{H−H−H−H}$$

To evaluate the validity of our calculations, we first performed calculations on the unadsorbed surface. The lowest unoccupied band had a 2px character localized on surface atoms, whereas the highest occupied band had a predominantly 2s and 2pz character. We also calculated the MESP for all the models. The MESP yields information on the molecular regions that are preferred or avoided by an electrophile or nucleophile. Any chemical system creates an electrostatic potential around itself; when a hypothetical "volumeless" unit positive charge is used as a probe, the probe feels attractive or repulsive forces in the regions where the electrostaic potential is negative or positive, respectively. Because we assume an atomic oxygen is interacting with the Si(100) surface, considerable attention has been paid to the potential map to locate the nucleophilic and electrophilic region to propose the possibility of an atomic oxygen interaction from the results obtained by periodic DFT calculation. The results of an exemplary case are shown in Figure 4. The MESP has been plotted in the region of −0.05 au to +0.05 au. For H−F−F−H there is a diamond-shaped −ve potential region just on top of F which may cause a hindrance in the penetration of atomic oxygen from top to react with the Si−Si bridge, i.e., the formation of Si−O−Si is impossible. The rest of the surface is surrounded by a +ve potential region. These findings can be extrapolated for other models of the types F−H−H−H, F−F−H−H, and H−F−H−F for comparison. Now, it seems obvious that the last one will have the highest probability of allowing atomic oxygen to interact with the bridging Si to create a Si−O−Si which is discussed in the later section. The stabilization energy results are tabulated in Table 1. The results show the Si(100) surface terminated as in the model H−F−H−F has the most stability compared with other possible models examined in this study. These results match the experimental prediction of alternate occurrence of fluorine on the Si(100) surface. An earlier study[46] using first-principle quantum mechanical calculations showed that the F atoms first attack the dangling bonds of dimers and

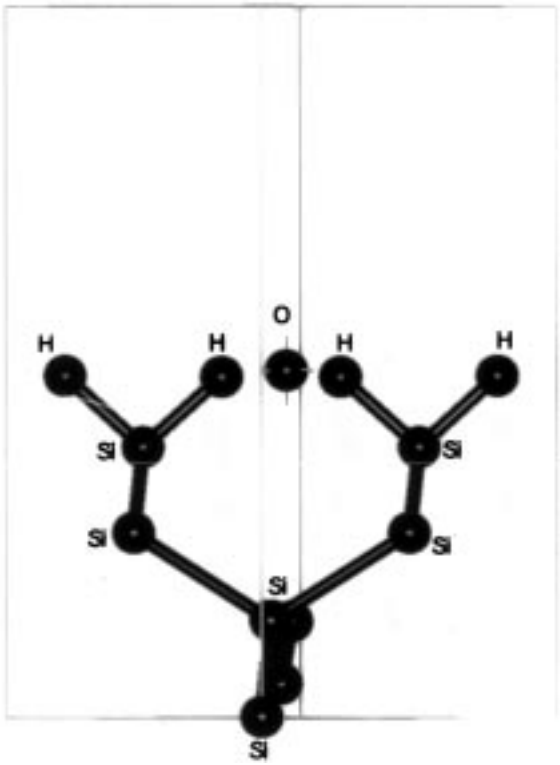

Figure 5. The model for atomic oxygen adsorption on the unreconstructed Si(100) surface.

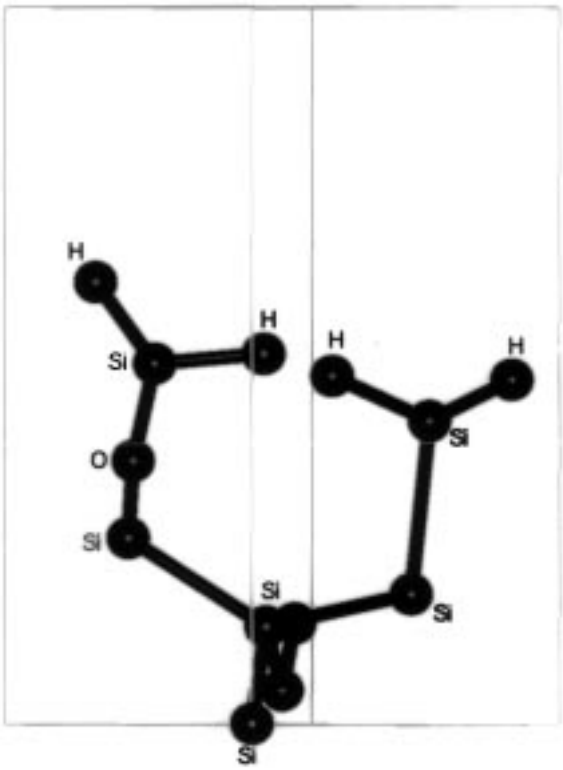

Figure 7. The optimized structure of the H-terminated unreconstructed Si(100) surface with oxygen insertion in the Si−Si back-bond.

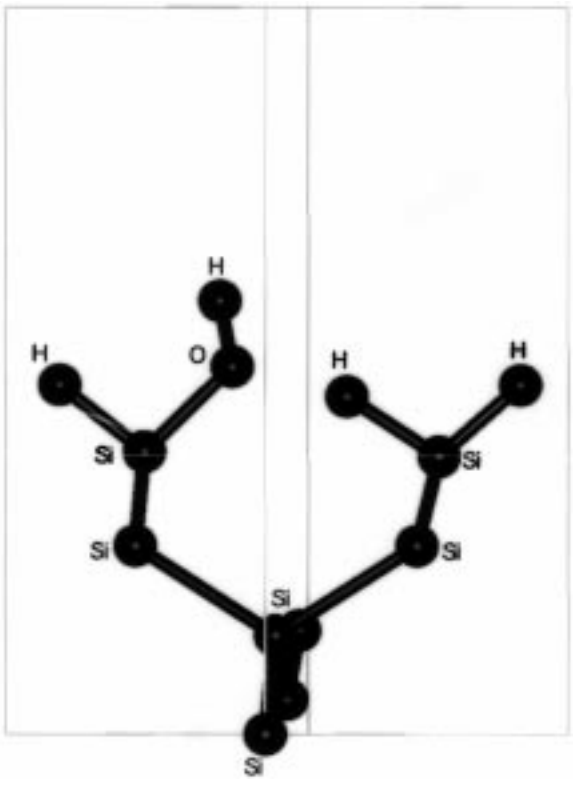

Figure 6. The optimized structure of H-terminated unreconstructed Si(100) surface with oxygen insertion in the Si−H bond.

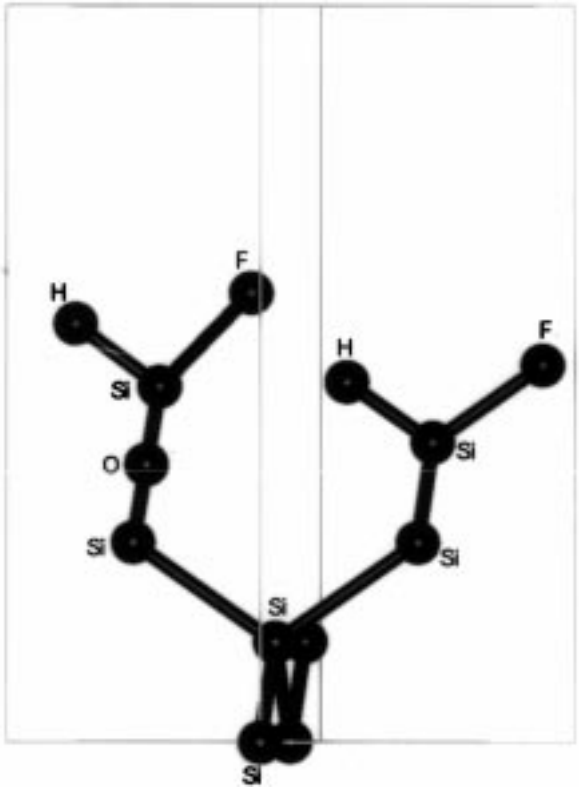

Figure 8. The optimized structure of F-terminated unreconstructed Si(100) surface (H−F−H−F) with oxygen insertion in the Si−Si back-bond.

saturate the surface with SiF species at lower F coverages. Formation of $SiF_{2(ad)}$ should occur only after all dangling bonds on the Si dimers are saturated. However, the repulsion between adjacent F increases with an increase in F coverage, making defluorination more difficult at higher coverage. The mechanism of fluorination starting from the monolayer to higher order layers is yet to be explored theoretically. Here we concentrate on the monolayer. This result will be confirmed further by the oxidation of the Si−Si bridging bond in the next section.

(c) Oxidation of the H- and F-Terminated Unreconstructed Si(100) Surface. Initial adsorption sites of O atom

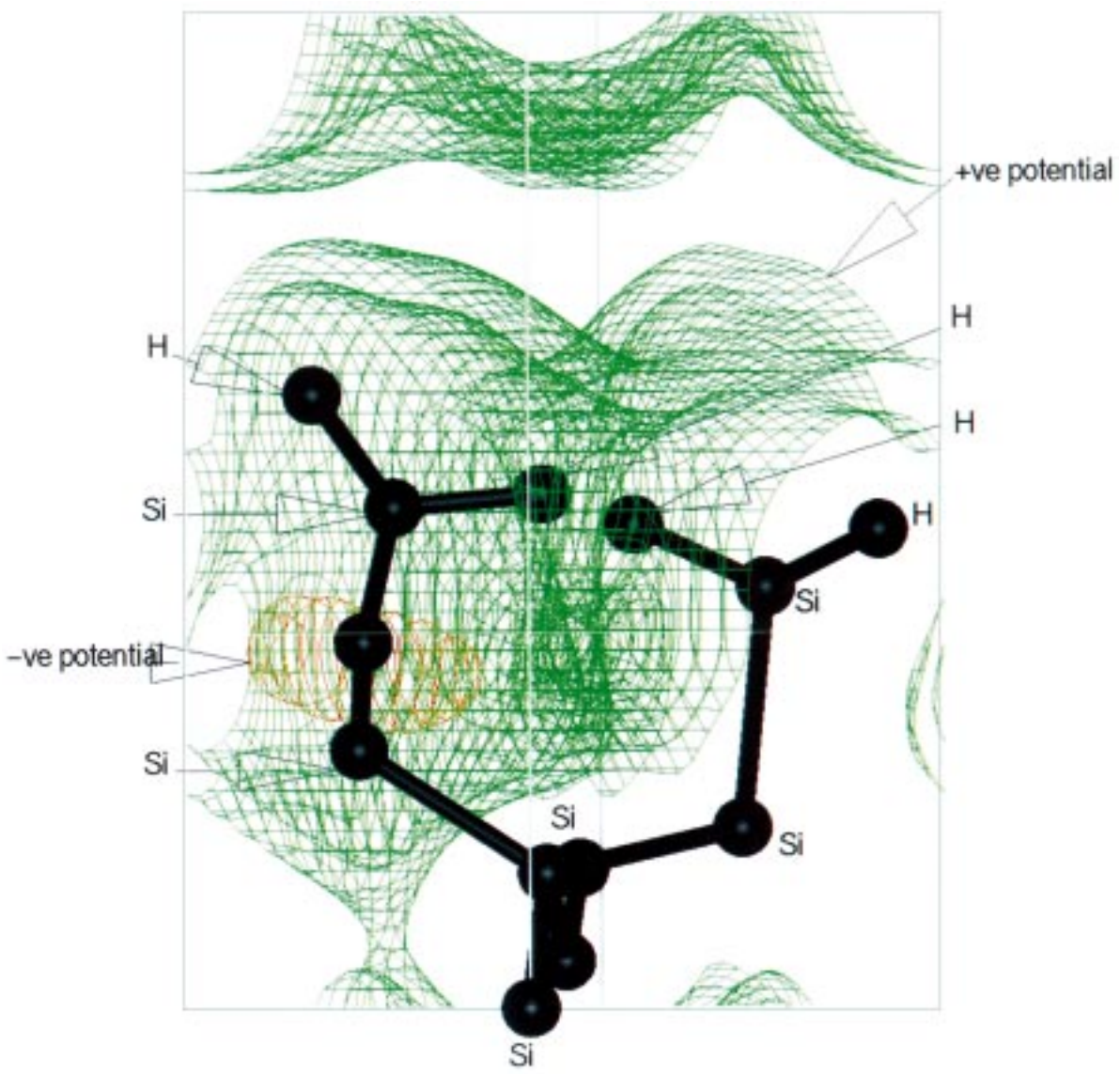

Figure 9. MESP map for the model of H-terminated unreconstructed Si(100) surface with oxygen insertion in Si−Si back-bond. The +ve and −ve potentials are shown as green and red shades, respectively. The −ve potential values in the range of −0.05 au to 0.00 au and the positive potentials in the range of 0.00 to 0.05 au are shown.

TABLE 2: Comparison of Total Energy and Adsorption Energy for Oxidation of the Respective Models of the Unreconstructed Si(100) Surface for Formation of Both Si−O−H and Si−O−Si

surface models	total energy (au)	adsorption energy (kcal/mol)
H−H−H−H (Si−O−H)	−49.92	21.2
H−H−H−H (Si−O−Si)	−51.91	23.8
F−H−H−H (Si−O−Si)	−55.30	24.2
H−F−H−F (Si−O−Si)	−61.33	29.8

TABLE 3: Adsorption Energy of Atomic Oxygen Adsorption over Cluster Models Mimicking the Surface Using DFT

mode of adsorption	Si−O	Si−Si	E (au)	ΔE (kcal/mol)
unreconstructed surface $\theta = 1$	1.55	3.84	−64.56	24.6
$H_3SiOSiH_3$	1.64	3.29	−27.82	104.3[a]
$H_2SiOSiH_2$				
singlet	1.65	3.29	−26.32	86.3[b]
triplet	1.64	3.29	−26.42	96.8[c]

[a] Relative to O and Si_2H_6 (−24.68 au). [b] Relative to O and SiH_2 (singlet) −25.22 au. [c] Relative to O and Si_2H_4 −26.28 au.

are Si−Si back-bonds and Si−H bonds for oxidation of H-terminated Si(100) surface.[47] In the oxidation of H-terminated Si(100) surfaces in air, the Si−H bonds are reported to be much more stable against oxidation than the Si−Si back-bonds.[48] These differences in the initial adsorption sites are considered to arise from the chemical activity of atomic oxygen. It is difficult to distinguish the oxygen adsorption from the oxide growth at large uptake. At low coverage, both atomic and molecular chemisorbed species have been found on Si(111) and Si(100) surfaces. On Si(100) surfaces, oxidation takes place near defects. We studied the adsorption of atomic oxygen on the Si(100) unreconstructed surface. The model is shown in Figure 5. The termination may be either H or F. To study the oxidation of the H-terminated surface we have chosen two possible locations of oxygen on the Si(100) surface. One is insertion of oxygen on the Si−H bond on the Si(100) surface resulting in the Si−O−H bridge and second is the insertion of oxygen in the Si−Si back-bond resulting in the Si−O−Si bridge. In both the cases the geometry was optimized for all the models as stated earlier. The respective optimized structures are shown

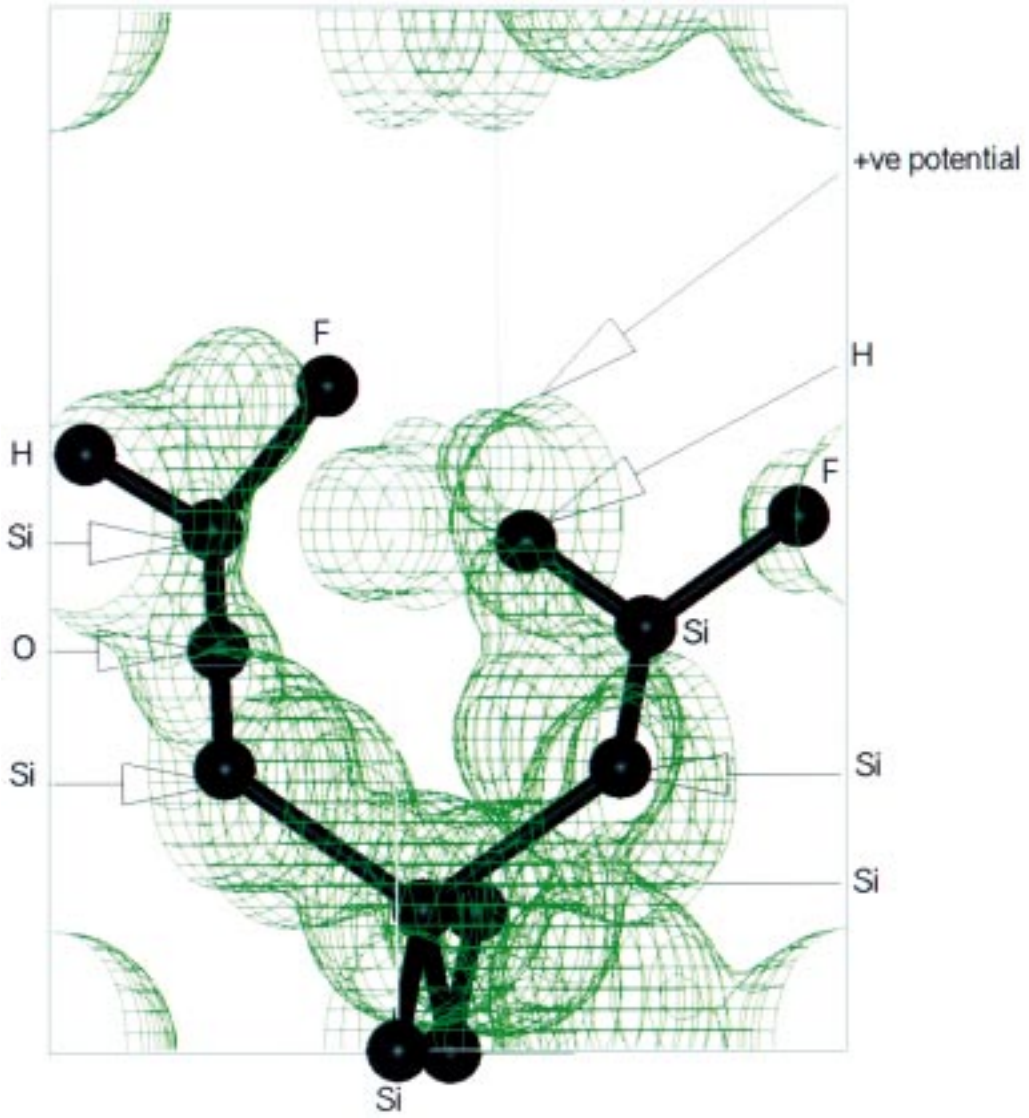

Figure 10. MESP map for the F-terminated unreconstructed Si(100) surface model H−F−H−F with oxygen insertion in the Si−Si back-bond. The +ve potentials are shown as green shade. The −ve potential did not occur. The positive potentials in the range of 0.00 to 0.05 au are shown.

in Figures 6 and 7. The adsorption energy was calculated by use of the following expression: $E_{ads} = E_O + E_{slab} - E_{(O+slab)}$. The results are shown in Table 2. The results show that first the Si(100) surface with the Si−O−Si bridge becomes more stabilized than that of Si−O−H. The oxygen insertion makes the Si−O distance 1.65 Å. The result again agrees with the experimental proposition, that after the insertion of oxygen in the Si−O−Si bridge the strain resulting from the insertion can be dissipated through the other Si bonds, whereas the surface insertion resulting in Si−O−H bond formation causes an unstability caused by the tendency of the other hydrogens of the surface to form hydrogen bonds. The model for oxygen insertion in the Si−Si back-bond for F-terminated surface is shown in Figure 8. In fluorine-terminated models, for the H−F−H−F model, the oxygen adsorption in the Si−Si back-bond to form the Si−O−Si bridge is a favorable process compared with the other respective models terminated with H, as shown in Table 2. In F-terminated surfaces, the oxidation of the Si−Si bridge results in a distortion of the surface, and the F seems to pull away from the rest of the surface resulting in an enhancement of the Si−O distance, i.e., 1.69 Å. The pull may be due to the interaction of two −ve moeties, i.e., O and F in a closer distance. This distortion paves the path for future study to see the number of oxygen incorporation in the Si−Si bridge and also to study the change in cell parameters by using pseudopotential quantum chemical periodic calculation methodology. This is also a limitation of the model; because we cannot mimic the oxidation process in the depth, it only accounts for the lateral insertion of the oxygen in the bridge, so we are unable at this point to predict the overall structural disorder. However, the adsorption energy still follows the order of the experiment. Most importantly, the H−F−H−F model shows greater stability after oxidation of the Si−Si back-bond than the H-terminated models. This justifies the experimental observation that oxidation is more favorable with fluorine termination on the Si(100) surface. This can be supported further by the MESP maps shown in Figures 9 and 10 for the oxidation of Si−Si back-bond present in both H-terminated (H−H−H−H) and F-terminated (H−F−H−F) models. It has been carried out also in the range of −0.05 au to +0.05 au. In case of atomic oxygen insertion in Si−Si back-bond for H-terminated surface the −ve potential still remains around the O site depicting an unsaturation in the surface, whereas in F-terminated surfaces it looks more stabilized, although the bond length of Si−O is increased a little bit. This can be confirmed only by analyzing the cell parameters, which is the aim of our future study.

(d) Model Calculations. These are the results of cluster calculations performed by DFT. First ,we tried to see the molecular oxygen adsorption on two types of models: one, monobonded SiH_3-SiH_3 and another, $SiH_2=SiH_2$. For the di-σ or "bridging peroxo" mode, each oxygen is bound to one Si atom. Each Si atom from the surface thus involves one dangling bond to build the Si−O bond. The Si−Si distance (3.84 Å) is close to the unreconstructed model. Here, the pz orbital interacts with the symmetric pair of dangling bonds (empty), and the pz* orbital interacts with antisymmetric pair of the Si dangling bonds (filled). The optimized structure is stable by 37.7 kcal/mol. However, it is not possible to transfer the staggered geometry for the adsorption; the motion of the O−O out of the *xz* plane is not allowed because the dangling bonds of the Si surface atoms lie in the *xz* plane. The higher energy of the eclipsed configuration of $Si_2H_6 + O_2$ is not favorable, so the molecular adsorption of oxygen on the unreconstructed surface is unlikely and our further study is related to adsorption of atomic oxygen on the Si surface. For the unreconstructed surface, the saturation of all the dangling bonds is only obtained at $\theta = 1$ coverage. The presence of two dangling bonds on each surface atom in the unreconstructed surface suggests bridging oxygen atoms. This therefore should correspond to the optimal situation, preceding the oxide growth. Because the surface atoms have two different orbitals, an unoccupied σ-orbital perpendicular to the surface and an empty p orbital parallel to the surface, we can also expect an asymmetric binding of an atomic oxygen with a surface atom (generating a Si=O species). For $\theta = 1/2$, the unreconstructed surface seems less attractive, and the dimerization obtained for the clean surface should survive. It has been postulated that the atomic oxygen occupies the short-bridge site between the first- and second-layer silicon atoms. This is impossible without an increase of the interlayer distance. We observed through our study that distance constraints prevent the insertion, and also that the adsorption of atomic oxygen atoms contribute to decreasing the overlap population between the Si atoms of the first and second layers. Referring to the SiH_2 model with a few filled (σz) and vacant (3px) orbitals, a single dangling bond cannot be isolated on the surface atom, then $H_2SiOSiH_2$ is a more appropriate model. When the Si−Si distance remains large, it is a biradical of ether type. In these two ether models the interaction energy is large (Table 3), especially for the triplet state of $H_2SiOSiH_2$. However, the optimal Si−Si distance, 3.39 Å, does not fit well the distances between the surface atoms. The cost for increasing this distance from 3.29 to 3.84 Å (as in the unreconstructed surface) is 38 kcal/mol.

When polarization functions are added to the system, the adsorption energy is increased in particular because the reference energy for the atomic oxygen is not affected, whereas that for adsorption is improved. The geometry of the adsorption mode is strongly perturbed. Thus the difference mostly represents a shift of all the binding energies to large values. So finally, the cluster calculations validate our periodic model and at the same time justify that atomic oxygen adsorption is the most reliable process to occur on the unreconstructed Si(100) surface.

Conclusion

Our calculation has its own limitation because of computational constraints. Calculation with a larger periodic slab model along with a calculation to analyze the change in cell parameters can improve the understanding of the mechanism of the whole process. But these things are suppressed by the novelty of the finding. This is the first periodic calculation to show the stability of the Si(100) surface after F incorporation. It is also rationalized that alternate occurrence of F on the unreconstructed surface results in a greater stability. The study to show oxidation was first validated by the cluster model; it shows that molecular oxygen adsorption on the surface is impossible, whereas atomic oxygen adsorption seems to be more realistic. The adsorption energy calculations for the periodic model suggest that in oxidation of the H-terminated surface the oxidation of the bridging Si bond, i.e., Si−O−Si, is more stable than Si−O−H. With F-terminated surface it shows that oxidation is more favorable in the presence of flourine on the surface than hydrogen. The results agree with the experimental observation and also justify the accountability of computer simulation techniques to explain the surface reaction mechanisms. This results are encouraging to propagate our further study in explaining the etching mechanism of fluorine on the Si(100) surface.

References and Notes

(1) Engel, T. *Surf. Sci. Rep.* **1993**, *18*, 91.
(2) Irene, E. A. *CRC Crit. Rev. Solid State Mater. Sci.* **1988**, *14*, 175.
(3) Sofield, C. J.; Stoneham, A. M. *Semicond. Sci. Technol*. **1995**, *10*, 215.
(4) Balk, P. *Mater. Sci. Monogr.* **1988**, *32*.
(5) Ohashi, M.; Hattori, T. *Jpn. J. Appl. Phys.* **1997**, *36*, L397.
(6) Ohmori, K.; Ikeda, H.; Iwano, H.; Zaima, S.; Yasuda, Y. *Appl. Surf. Sci.* **1997**, *117*/*118*, 114.
(7) Ikeda, H.; Nakagawa, Y.; Toshima, M.; Furuta, S.; Zaima, S.; Yasuda, Y. *Appl. Surf. Sci.* **1997**, *117*/*118*, 109.
(8) Himpsel, F. J.; McFeely, F. R.; Talab-Ibrahimi, A.; Yarmoff, J. A.; Hollinger, G. *Phys. Rev. B* **1988**, *38*, 6084.
(9) Ciraci, S.; Ellialtioglu, S.; Erkoe, S. *Phys. Rev. B* **1982**, *26*, 5716.
(10) Hofer, U.; Morgan, P.; Wurth, W.; Umbach, E. *Phys. Rev. Lett.* **1985**, *55*, 2979.
(11) Chan, M.; Batra, I. P.; Brandle, C. R. *J. Vac. Sci. Technol.* **1979**, *16*, 1216.
(12) Kunjunney, T.; Ferry, D. K. *Phys. Rev. B* **1981**, *24*, 4593.
(13) Ellialtioglu, S.; Ciraci, S. *Solid State Commun.* **1982**, *42*, 869.
(14) Schaefer, J. A.; Stucki, F.; Frankel, D. J.; Gopel, W.; Lapeyre, G. J. *J. Vac. Sci. Technol. B.* **1984**, *2*, 359.
(15) Schaefer, J. A.; Gopel, W. *Surf. Sci.* **1985**, *155*, 535.
(16) Genzebrock, F. H.; Babasaki, Y.; Tanaka, M.; Nakamura, T.; Namiki, A. *Surf. Sci.* **1993**, *297*, 141.
(17) Coburn, J. W.; Winters, H. F. *Annu. Rev. Mater. Sci.* **1983**, *13*, 91.
(18) Chuang, T. J. *J. Appl. Phys.* **1980**, *51*, 2614.
(19) Mucha, J. A.; Donnelly, V. M.; Flamm, D. L.; Webb, L. M. *J. Phys. Chem.* **1981**, *85*, 3529.
(20) Gruntz, K. J.; Ley, L.; Johnson, R. L. *Phys. Rev. B* **1981**, *24*, 2069.
(21) Coburn, J. W.; Chen, M. *J. Appl. Phys.* **1980**, *51*, 3134.
(22) Shinn, N. D.; Morar, J. F.; McFeely, F. R. *J. Vac. Sci. Technol.* **1984**, *A2*, 1593.
(23) Stinespring, C. D.; Freedman, A. *Appl. Phys. Lett.* **1986**, *48*, 718.
(24) McFeely, F. R.; Morar, J. F.; Himpsel, F. *J. Surf. Sci.* **1986**, *165*, 277.
(25) Winters, H. F.; Coburn, J. W.; Chuang, T. J. *J. Vac. Sci. Technol.* **1983**, *B1*, 469.
(26) Engstrom, J. R.; Nelson, M. M.; Engel, T. *Surf. Sci.* **1989**, *215*, 437.
(27) Aoyama, T.; Yamazaki, T.; Ito, T. *Appl. Phys. Lett.* **1991**, *59*, 2577.
(28) Aliev, V. S.; Kruchinin, V. N.; Baklanov, M. R. *Surf. Sci.* **1996**, *347*, 97.
(29) Weakleim, P. C.; Wu, C. J.; Carter, E. A. *Phys. Rev. Lett.* **1992**, *69*, 200.
(30) Weakleim, P. C.; Carter, E. A. *J. Chem. Phys.* **1993**, *98*, 737.
(31) Dsolid User Guide, MSI, Sandiego, October 1995.
(32) Kohn, W.; Sham, L. J. *Phys. Rev. A* **1965**, *140*, 1133.
(33) Vosko, S. H.; Wilk, L.; Nusair, M. *Can. J. Phys.* **1980**, *58*, 1200.
(34) Delley, B. *J. Chem. Phys.* **1990**, *92*, 508.
(35) Velde, G. te.; Baerends, E. J. *Phys. Rev. B* **1991**, *44*, 7888.
(36) Ewald, P. P. *Ann. Phys.* **1921**, *64*, 253.
(37) Delley, B. *J. Phys. Chem.* **1996**, *100*, 6107.
(38) Vetrivel, R.; Deka, R. C.; Chatterjee, A.; Kubo, M.; Broclawik, E.; Miyamoto, A. *Theor. Comput. Chem.* **1996**, *3*, 509.

(39) Uhrbarg, R. I. G.; Hansson, G. V., Flodstrom, J. M. *Phys. Rev. B* **1981**, *24*, 4684.
(40) Zhu, Z.; Shima, N.; Tsukada, M. *Phys. Rev. B* **1989**, *24*, 2303.
(41) Roberts, N.; Needs, R. J. *Surface Sci.* **1990**, *236*, 112.
(42) Silvi, B.; Fourati, N.; Nada, R.; Catlow, C. R. A. *J. Phys. Chem. Solids* **1991**, *52*, 1005.
(43) Fahmi, A.; Minot, C., Silvi, B.; Causa, M. *Phys. Rev. B* **1993**, *47*, 11717.
(44) Becke, A. D. *J. Chem. Phys.* **1993**, *98*, 1372.
(45) Curtiss, L. A.; Raghavachari, K.; Pople, J. A. *J. Chem. Phys.* **1993**, *98*, 1293.
(46) Wu, C. J.; Carter, E. A. *Phys. Rev. B* **1992**, *45*, 9065.
(47) Ikeda, H.; Hotta, K.; Yamada, T.; Zaima, S.; Iwano, H.; Yasuda, Y. *J. Appl. Phys.* **1995**, *77*, 5125.
(48) Takahagi, T.; Ishitani, A.; Kuroda, H. *J. Appl. Phys.* **1990**, *68*, 2187.